

# Anticancer Effects of ZnO/CNT@Fe<sub>3</sub>O<sub>4</sub> in AML-Derived KG1 Cells: Shedding Light on Promising Potential of Metal Nanoparticles in Acute Leukemia

Amir-Mohammad Yousefi<sup>1</sup>, Atieh Pourbagheri-Sigaroodi<sup>2</sup>, Zahra Fakhroueian<sup>3</sup>, Sina Salari<sup>4</sup>, Kosar Fateh<sup>2</sup>, Majid Momeny<sup>5</sup>, Davood Bashash<sup>2</sup>

<sup>1</sup>Student Research Committee, Department of Hematology and Blood Banking, School of Allied Medical Sciences, Shahid Beheshti University of Medical Sciences, Tehran, Iran

<sup>2</sup>Department of Hematology and Blood Banking, School of Allied Medical Sciences, Shahid Beheshti University of Medical Sciences, Tehran, Iran

<sup>3</sup>School of Chemical Engineering, College of Engineering, Institute of Petroleum Engineering, University of Tehran, Tehran, Iran

<sup>4</sup>Department of Medical Oncology, Hematology and Bone Marrow Transplantation, Taleghani Hospital, Shahid Beheshti University of Medical Sciences, Tehran, Iran

<sup>5</sup>Turku Centre for Biotechnology, University of Turku and Åbo Akademi University, Turku, Finland

**Corresponding Author:** Davood Bashash, Department of Hematology and Blood Banking, School of Allied Medical Sciences, Shahid Beheshti University of Medical Sciences, Tehran, Iran

**Tel:** +98-21-22717504

**Fax:** +98-21-22721150

**E-mail:** D.bashash@sbmu.ac.ir

Received: 24, Jul, 2020

Accepted: 07, Oct, 2021

## ABSTRACT

**Background:** Therapeutic approaches for acute myeloid leukemia (AML) have remained largely unchanged for over 40 years and cytarabine and an anthracycline (e.g., daunorubicin) backbone is the main induction therapy for these patients. Resistance to chemotherapy is the major clinical challenge and contributes to short-term survival with a high rate of disease recurrence. Given the established efficacy of nanoparticles in cancer treatment, this study was designed to evaluate the anticancer property of our novel nanocomposite in the AML-derived KG1 cells.

**Materials and Methods:** To assess the anti-leukemic effects of our nanocomposite on AML cells, we used MTT and trypan blue assays. Flow cytometric analysis and q-RT-PCR were also applied to evaluate the impact of nanocomposite on cell cycle and apoptosis.

**Results:** Our results outlined that ZnO/CNT@Fe<sub>3</sub>O<sub>4</sub> decreased viability and metabolic activity of KG1 cells through induction of G1 arrest by increasing the expression of p21 and p27 cyclin-dependent kinase inhibitors and decreasing c-Myc transcription. Moreover, ZnO/CNT@Fe<sub>3</sub>O<sub>4</sub> markedly elevated the percentage of apoptotic cells which was coupled with a significant alteration of Bax and Bcl-2 expressions. Synergistic experiments showed that ZnO/CNT@Fe<sub>3</sub>O<sub>4</sub> enhances the cytotoxic effects of Vincristine on KG1 cells.

**Conclusion:** In conclusion, this study sheds light on the potent anti-leukemic effects of ZnO/CNT@Fe<sub>3</sub>O<sub>4</sub> and provides evidence for the application of this agent in the treatment of acute myeloid leukemia.

**Keywords:** Acute myeloid leukemia (AML); Zinc oxide; Carbon nanotubes; Iron oxide; Nanoparticles; Vincristine

## INTRODUCTION

Treatment of cancer has become more aggressive during the current years and severe side effects have

called into question the recent advances in this field<sup>1</sup>.

As one of the most prevalent leukemia in older adults and the fifth most common malignancy in children,

Copyright © 2022 Tehran University of Medical Sciences. This work is licensed under a Creative Commons Attribution-Noncommercial 4.0 International license (<http://creativecommons.org/licenses/by-nc/4.0>). Non-commercial uses of the work are permitted, provided the original work is properly cited.

acute myeloid leukemia (AML) affects about 21,450 people in the United States and resulted in 10,920 deaths in 2019<sup>2,3</sup>. The present status of therapeutic approaches for this malignancy has demonstrated low levels of hope at the end of treatment, and a great number of AML patients will relapse after initial promising response<sup>4</sup>. Moreover, severe side effects of conventional chemotherapy highlight the necessity of novel compounds that more effectively kill the tumor cells while exhibiting the least toxicity towards normal tissues<sup>5</sup>.

The application of nanomaterials is one of the most hopeful approaches to provide a promising solution to meet these challenges<sup>6</sup>. Nowadays, many publications have evaluated the application of different types of metal nanoparticles in a wide range of biomedical and medical areas. ZnO quantum dots (QDs) and Fe<sub>3</sub>O<sub>4</sub> nanoparticles (NPs) were the most promising nanomaterials in which their anti-cancer effects have been proved in a broad spectrum of tumors<sup>7,8</sup>. It has been reported that ZnO NPs could decrease the viability of CAL-27<sup>9</sup>, U87<sup>10</sup>, and MCF-7<sup>11</sup> cell lines. Yuexia Xie et al. indicated that Fe<sub>3</sub>O<sub>4</sub> NPs induce significant cytotoxic effects in two kinds of human hepatoma cell lines, SK-Hep-1 and Hep3B, mainly through mitochondria-dependent ROS generation<sup>12</sup>. Tanino et al. reported that ZnO NPs exert significant cytotoxicity against lung cancer cells while they exhibited less cytotoxic effects on normal lung-derived cells and did not elicit observable adverse effects after intravenous administration<sup>13</sup>. The results of our recent study have demonstrated that ZnO/CNT@Fe<sub>3</sub>O<sub>4</sub> significantly reduced the survival of CML-derived K562 cells through ROS generation and alteration of apoptosis-related genes<sup>14</sup>. The prominent efficacy of NPs against chronic myeloid leukemia cells and the lack of an efficient treatment in acute leukemia encouraged us to investigate whether ZnO/CNT@Fe<sub>3</sub>O<sub>4</sub> induces favorable cytotoxicity in AML cells. To this end, KG1 cells were subjected to various concentrations of ZnO/CNT@Fe<sub>3</sub>O<sub>4</sub>, and then cell viability index, metabolic activity, growth kinetics, and transcriptional alteration of apoptosis- and cell cycle-related genes were investigated to dissect the underlying mechanisms by which ZnO/CNT@Fe<sub>3</sub>O<sub>4</sub> exert its cytotoxic effect.

## Materials and Methods

### Synthesis and formulation of nanocomposite

Briefly, 0.5-2 gr ZnO nanoparticles (coated with hydrophilic CNT@fatty) and iron oxide NPs were used to modify 1-3 gr multiwall CNT (8-15 nm) in 20 ml pure ethanol. As synergic material, 1-2 gr zinc oxide NPs powder was added to nanofluid and the components were mixed at room temperature. Afterward, 1-2 gr PEG 6000 as a binding agent was added and the mixture was stirred at 40-50 °C for 1-2 h. Then, 2-3 ml Span 80 as a stabilizer, emulsifier, and nonionic surfactant was added with persistent vigorous stirring, under reflux processing in about 2 h duration of the reaction.

### Cell lines and drug treatments

To investigate the impact of ZnO/CNT@Fe<sub>3</sub>O<sub>4</sub> on acute myeloid leukemia, KG-1 cells were grown in suspension in RPMI 1640 medium supplemented with 2 mM L-glutamine and 10% heat-inactivated fetal bovine serum. The cell cultures were all kept at 37 °C in a humidified atmosphere of 5% CO<sub>2</sub>. The leukemic cells were then treated with the relevant amounts of ZnO/CNT@Fe<sub>3</sub>O<sub>4</sub>, Vincristine (VCR) (Sina Daroo, Iran), and the combination of both agents. KG1 cells were also exposed to equal amounts of solvents, as an alternative control at the final concentration of 0.1%.

### Trypan blue exclusion assay

Trypan blue assay was tested on 150 × 10<sup>3</sup> leukemic cells seeded in a 24-well plate in the medium containing different concentrations of ZnO/CNT@Fe<sub>3</sub>O<sub>4</sub>, either as a single agent or in combination with VCR. Following the indicated time intervals, centrifuged cell pellets were re-suspended in serum-free complete medium, and then an equivalent amount of 0.4% trypan blue was added to each sample. The numbers of viable cells were counted manually under a light microscope and the percentage of viable cells was assessed.

### Detection of metabolic activity by microculture tetrazolium test

Acute myeloid leukemia cells (5 × 10<sup>3</sup>) were seeded in 96-well plate in the presence of ZnO/CNT@Fe<sub>3</sub>O<sub>4</sub>, as a single agent or in combined-modality with VCR,

and incubated in a humidified 5% CO<sub>2</sub> incubator at 37 °C. The experiment process has been described in our previous article <sup>15</sup>.

#### **Determination of combination index (CI) and dose reduction index (DRI)**

To investigate the efficacy of agent combinations, the reduction of cell survival was examined, and the combination index (CI) and dose reduction index (DRI) were evaluated as described previously <sup>16</sup>. The CI values of <1, =1, and >1 indicate synergism, additive effect, and antagonism of agents, respectively.

#### **RNA extraction, cDNA synthesis, and quantitative real-time PCR**

Total RNA from AML-derived KG1 cells was extracted using the RNA Isolation Kit (Roche, Mannheim, Germany). After confirming the quantity of the extracted RNA by Nanodrop instrument, the reverse transcription reaction was performed using a cDNA synthesis kit (Takara Bio, Shiga, Japan). Next, to examine the effect of ZnO/CNT@Fe<sub>3</sub>O<sub>4</sub>/VCR on the expression of proliferation- and apoptotic-related genes, cDNAs were subjected to quantitative real-time PCR (qRT-PCR). The fold change values were calculated based on the  $2^{-\Delta\Delta Ct}$  relative expression formula.

#### **Assessment of cell distribution in the cell cycle using flow cytometry**

The impact of ZnO/CNT@Fe<sub>3</sub>O<sub>4</sub>-plus-VCR on the cell cycle progression was evaluated by PI staining. After the treatment of KG1 cells with the designated concentrations of agents, either alone or in combination, the cells were harvested, washed with cold PBS, and then fixed in 70% ethanol overnight. Afterward, for DNA staining and RNA degradation, we added PI and RNase, respectively. Cells were then incubated for a further 30 min, and the distribution of cells was evaluated by flow cytometry. For interpreting the obtained data, we used the Windows FlowJo V10 software.

#### **Detection of apoptosis using flow cytometry**

To investigate the effect of ZnO/CNT@Fe<sub>3</sub>O<sub>4</sub> on the induction of programmed cell death, AML cells were subjected to apoptosis analysis. Briefly, after 24h of treatment with the designated concentrations of ZnO/CNT@Fe<sub>3</sub>O<sub>4</sub> in the presence or absence of VCR, KG1 cells were harvested, washed with PBS, and re-suspended in a total volume of 100 μl of the incubation buffer. After that, Annexin-V-Fluor (2 μl per sample) was added, and cell suspensions were incubated for 20 min in the dark and then fluorescence was quantified using flow cytometry. Annexin V-positive and PI-negative cells were considered to be in the early apoptotic phase and cells having positive staining both for Annexin-V and PI were considered to undergo late apoptosis or necrosis.

#### **Statistical analysis**

Data were expressed as the mean ± standard deviation (S.D.) of three independent experiments. All presented data were analyzed using GraphPad Prism Software using a two-tailed student's test and one-way variance analysis. To compare the control group and the drugs-treated ones, Dennett's multiple comparison test was used. A probability level of  $P < 0.05$  was considered statistically significant.

## **RESULTS**

### **Characterization techniques of the synthesized ZnO/CNT@Fe<sub>3</sub>O<sub>4</sub> nanocomposite product**

ZnO/CNT@Fe<sub>3</sub>O<sub>4</sub> nanocomposite has been synthesized and its formulation and structure were examined by various characterization methods such as FTIR analysis, X-ray powder diffraction (XRD), scanning electron microscopy (SEM), and transmission electron microscopy (TEM). As presented in Figure 1, FTIR Spectrum of ZnO/CNT@Fe<sub>3</sub>O<sub>4</sub> indicated high-intensity broadband at 3402 which is related to the vibration mode of the hydroxyl group in water and carboxylic acid groups belonging to fatty acid in nanoparticle <sup>17</sup>. Symmetrical stretching vibration in 838 cm<sup>-1</sup> and 721 cm<sup>-1</sup> is associated with the presence of Zn-O and Fe-O in nanoformulation. Two low-intensity peaks observed at 1462 cm<sup>-1</sup> and 1399 cm<sup>-1</sup> are related to

symmetric and asymmetric -CH<sub>3</sub> groups respectively, which confirm the presence of polyethylene glycol (PEG) in the system<sup>18,19</sup>. At least two absorption peaks correlated to CNT were observed at 1110 cm<sup>-1</sup>, 1735 cm<sup>-1</sup> and 1645 cm<sup>-1</sup> that correspond to C-O-C<sup>20, 21</sup>, C = O<sup>22, 23</sup> and C = C, respectively<sup>24</sup>. X-ray diffraction peaks were in agreement with the results of the FTIR spectrum, where the standard XRD patterns of zinc oxide (JCPDS no.: 017-751377) and iron oxide magnetic nanoparticles (JCPDS no: 00-003-0863) confirmed the presence of aforementioned nanoparticles in the system. Moreover, the detected peak located at  $2\theta = 24.5$  could be indexed as (002) planes of CNT<sup>25</sup>. FESEM micrographs confirmed the formation of nanocomposite and revealed that there are individual particles on the surface of carbon nanotubes. Consistently, transmission electron microscopy (TEM) illustrated nanostructures composed mainly of nanorods, besides a few nano granules with diameters ranging from 5 to 80 nm.

#### **Inhibitory effects of ZnO/CNT@Fe<sub>3</sub>O<sub>4</sub> on viability and metabolic activity of KG1 cells**

Chemotherapy is not curative most of the time and has various complications, such as high toxicity and low specificity, emphasizing the necessity of incorporation of new therapeutic agents in AML<sup>26</sup>. To evaluate the effects of the newly synthesized nanocomposite on acute leukemia, KG1 cells were treated with the designated concentrations of ZnO/CNT@Fe<sub>3</sub>O<sub>4</sub>, and trypan blue exclusive assay and MTT assays were applied to evaluate the viability and metabolic activity, respectively. The results of time and concentration-dependent experiments demonstrated that both viability and metabolic activity declined upon exposure of KG1 cells to ZnO/CNT@Fe<sub>3</sub>O<sub>4</sub>. As demonstrated in Figure 2, while ZnO/CNT@Fe<sub>3</sub>O<sub>4</sub> at low concentrations exerted a minimal effect on KG1 cells, maximal repression was observed at 20 µg/ml where viability and metabolic activity decreased to 57% and 46%, respectively.

#### **ZnO/CNT@Fe<sub>3</sub>O<sub>4</sub> disrupts Bcl-2 and Bax transcription ratio in favor of apoptosis**

A growing body of evidence demonstrated that metal nanoparticles decrease the survival of cancer

cells through induction of apoptosis<sup>27</sup>. As a result, it was of great attention to assess whether the antileukemic properties of ZnO/CNT@Fe<sub>3</sub>O<sub>4</sub> in KG1 cells were because of the induction of apoptosis. The apoptotic effect of the compound against KG1 cells was confirmed by Annexin-PI staining, as we found a vigorous increase in both Annexin- and Annexin/PI-positive cells. To shed light on ZnO/CNT@Fe<sub>3</sub>O<sub>4</sub>-induced apoptosis at the molecular level, we analyzed the mRNA levels of Bcl-2 and Bax. As indicated in Figure 3, results of qRT-PCR demonstrated that not only ZnO/CNT@Fe<sub>3</sub>O<sub>4</sub> repressed the expression of Bcl2 also exerted a robust increase in mRNA level of Bax, indicating that ZnO/CNT@Fe<sub>3</sub>O<sub>4</sub> induces its apoptotic effect through disturbing the balanced ratio of Bax and Bcl2 genes.

#### **ZnO/CNT@Fe<sub>3</sub>O<sub>4</sub> induced its suppressive effects through ceasing KG1 cells in the G1 phase of the cell cycle**

Based on the considerable anti-proliferative effects of ZnO/CNT@Fe<sub>3</sub>O<sub>4</sub> on KG1 cells, which was proved by a substantial reduction in the number of NP-treated KG1 cells, it was interesting to determine whether this growth suppressive effect was coupled with alteration in the cell cycle. As presented in Figure 4, the effect of ZnO/CNT@Fe<sub>3</sub>O<sub>4</sub> on cell cycle distribution was investigated using PI staining, where we found that ZnO/CNT@Fe<sub>3</sub>O<sub>4</sub> augmented the fraction of hypodiploid cells in the sub-G1 phase, which is a representative of DNA fragmentation-mediated apoptosis in KG1 cells. We also found a noticeable rise in the percentage of the cells in G1 in a concentration-dependent manner. Furthermore, DNA content analysis showed that the population of ZnO/CNT@Fe<sub>3</sub>O<sub>4</sub>-treated cells was significantly diminished in the S phase of the cell cycle. Investigating the molecular mechanisms responsible for this effect demonstrated a robust increase in the mRNA expression levels of both p21 and p27, which can impede cell cycle progression through inhibition of CDKs. In congruence, the expression of c-Myc proto-oncogene which induces positive cell-cycle regulators was remarkably decreased in a concentration-dependent manner.

### Combination of ZnO/CNT@Fe<sub>3</sub>O<sub>4</sub> and VCR reduced the survival of KG1 cells synergistically

Given the potent antileukemic effects of our synthesized nanoparticle, it was enticing to evaluate the interaction between ZnO/CNT@Fe<sub>3</sub>O<sub>4</sub> and VCR, as one of the most common chemotherapeutic agents used in AML. While VCR at the concentration of 2 nM had slight effects on KG1 cells, its combination with ZnO/CNT@Fe<sub>3</sub>O<sub>4</sub> notably decreased the viability and metabolic activity. The results of isobologram analysis and combination index (CI) showed that ZnO/CNT@Fe<sub>3</sub>O<sub>4</sub> at the concentrations of 15 µg/ml and 20 µg/ml in combination with VCR synergistically decreased cell

viability. As presented in Fig.5, all the points are below the line of additive effects showing a synergistic effect between these agents. Our results were also confirmed by the fraction-affect (FA) versus combination index (CI) plot that exhibits a synergistic cytotoxic effect (CI < 1) in the combination treatment. Stimulatory effects of ZnO/CNT@Fe<sub>3</sub>O<sub>4</sub> on VCR cytotoxicity were further confirmed by apoptosis analysis, where we found that the percentage of both Annexin and Annexin/PI-positive cells were significantly higher in combinatorial series, indicating that ZnO/CNT@Fe<sub>3</sub>O<sub>4</sub> elevated the cytotoxicity of VCR through induction of apoptosis.

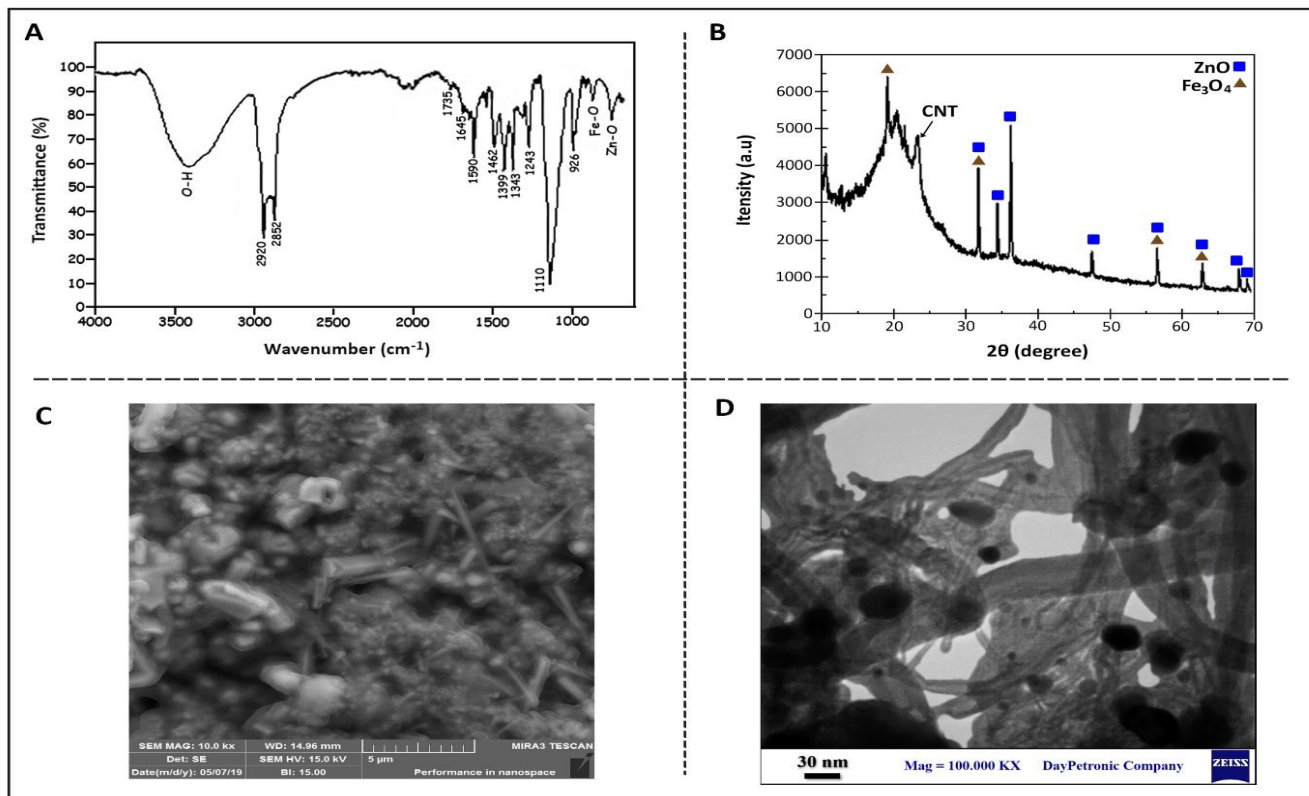


Figure 1 **A)** FTIR spectrum of ZnO/CNT@Fe<sub>3</sub>O<sub>4</sub> demonstrated characteristic peaks of Zn–O and Fe–O bonds at 721 and 834 cm<sup>-1</sup>, respectively. **B)** XRD analysis of ZnO/CNT@Fe<sub>3</sub>O<sub>4</sub> confirmed the structural characteristics of ZnO/CNT@Fe<sub>3</sub>O<sub>4</sub>. **C)** Attachment of round shaped Q-dot ZnO and Fe<sub>3</sub>O<sub>4</sub> NPs to CNTs was confirmed by scanning electron microscopy (SEM). **D)** Transmission electron microscopy (TEM) showed the morphology of the ZnO/CNT@Fe<sub>3</sub>O<sub>4</sub> nanocomposites and the maximum size of nanoparticles was determined by about 80 nm.

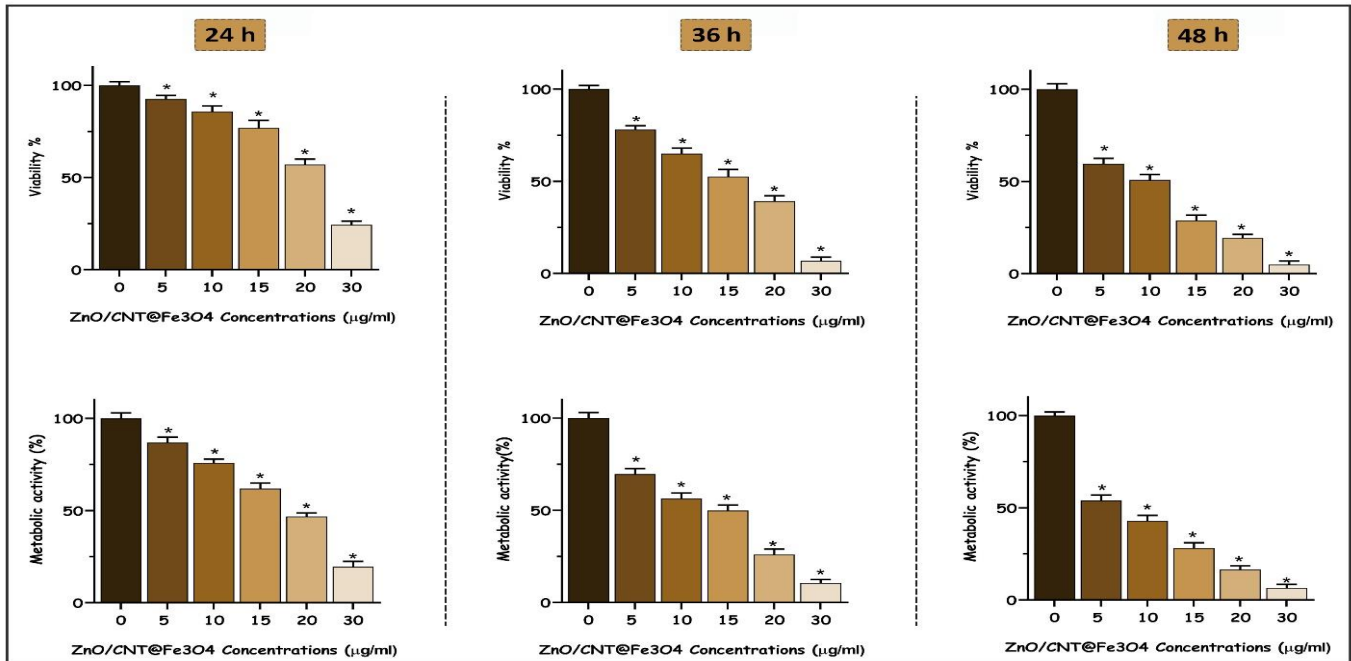


Figure 2. ZnO/CNT@Fe<sub>3</sub>O<sub>4</sub> decreased both viability and metabolic activity of KG1 cells. KG1 cells were treated with nanocomposite for 24 h, 36 h, and 48 h and cell viability and metabolic activity were evaluated by trypan blue exclusion and MTT assays, respectively. As presented, ZnO/CNT@Fe<sub>3</sub>O<sub>4</sub> reduced the survival of KG1 cells in concentration- and time-dependent manners. Values are given as mean ± S.D. of three independent experiments. \**P* ≤ 0.05 represented significant changes from the control.

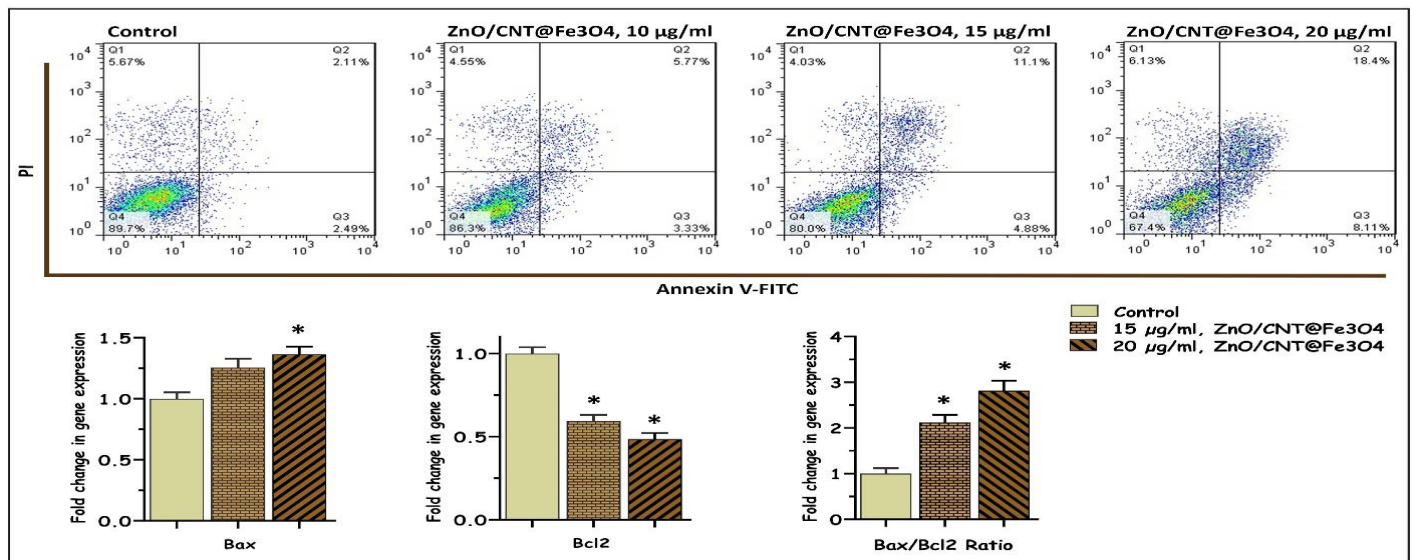


Figure 3. The apoptotic effects of ZnO/CNT@Fe<sub>3</sub>O<sub>4</sub> on KG1 cells. ZnO/CNT@Fe<sub>3</sub>O<sub>4</sub> increased the percentage of Annexin-V positive cells. The results of the qRT-PCR analysis revealed that ZnO/CNT@Fe<sub>3</sub>O<sub>4</sub> induced apoptosis, at least partly, through the alteration of the Bax/Bcl2 ratio. Values are given as mean ± standard deviation of three independent experiments. \**P* ≤ 0.05 represents significant changes from untreated control.

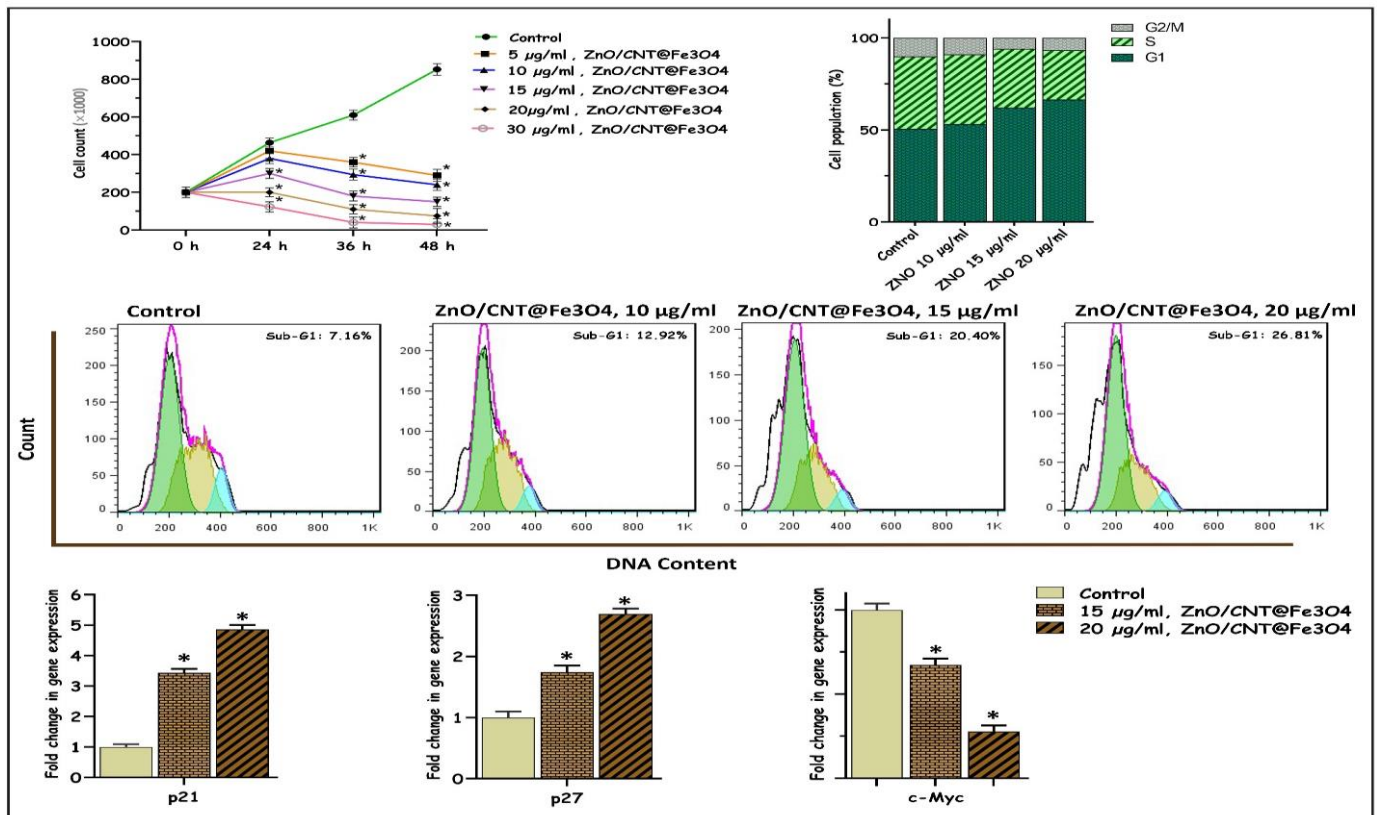


Figure 4. Our results revealed that ZnO/CNT@Fe<sub>3</sub>O<sub>4</sub> diminished the proliferative capacity of the cells, as evidenced by the decreased number of KG1 cells, via the induction of G1 cell cycle arrest. While the mRNA expression levels of p21 and p27 were increased upon exposure to the agent in a concentration-dependent manner, c-Myc transcription was decreased significantly. Values are given as mean  $\pm$  S.D. of three independent experiments. \**P*  $\leq$  0.05 represented significant changes from the control.

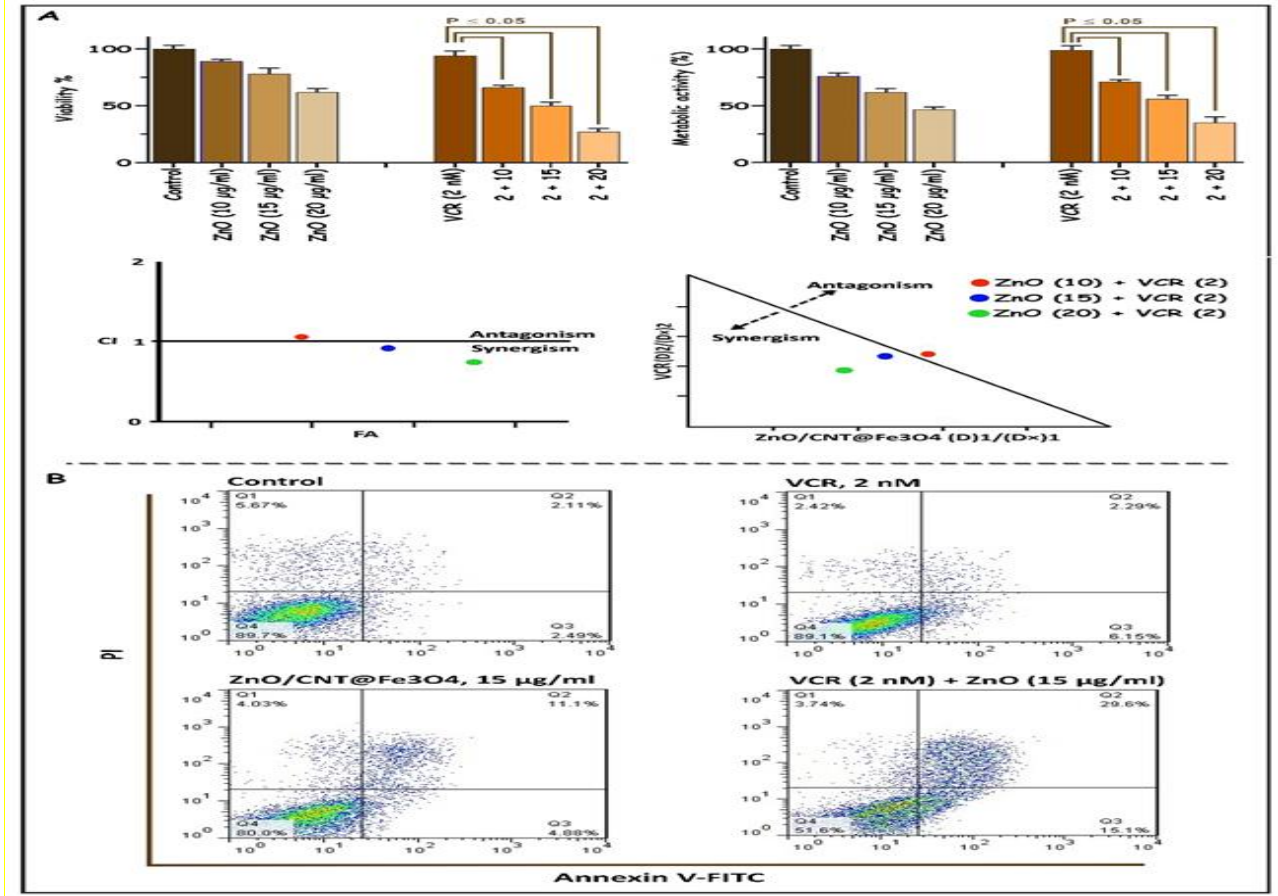


Figure 5. A) Combination of nanocomposite and VCR was more effective in reducing the survival of KG1 cells in comparison to each agent alone. The combination index (CI) was calculated according to the classic isobologram equation and the results revealed that ZnO/CNT@Fe<sub>3</sub>O<sub>4</sub> at the concentrations of 15 µg/ml and 20 µg/ml and VCR reduced the viability of KG1 cells in a synergistic manner. Points above and below the iso-effect line reflect antagonism and synergism, respectively. B) The result of the Annexin-PI assay further confirmed the synergistic interaction between nanocomposite and VCR. Values are given as mean ± S.D. of three independent experiments. \*P ≤ 0.05 represented significant changes from the control.

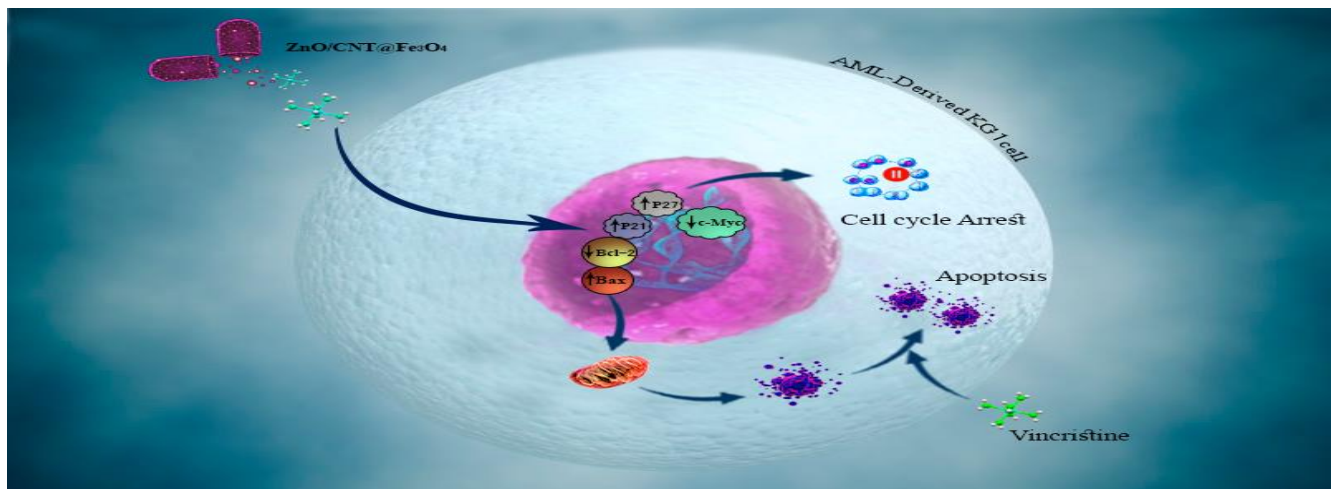


Figure 6. Schematic illustration proposed for the probable mechanism of action of ZnO/CNT@Fe<sub>3</sub>O<sub>4</sub> in KG1 cells. Not only ZnO/CNT@Fe<sub>3</sub>O<sub>4</sub> through alteration of the Bax-to-Bcl2 ratio induced apoptosis also exerted its antiproliferative effects on KG1 cells mainly through a p21- and p27-mediated G1 cell cycle arrest. Synergistic experiments also showed that the combination of ZnO/CNT@Fe<sub>3</sub>O<sub>4</sub> and VCR could synergistically elevate apoptotic cell death in AML-derived KG1 cell line.

## DISCUSSION

Therapeutic tactics for the treatment of AML remained unchanged for approximately 40 years and most of the patients will ultimately develop resistance and relapse<sup>28,29</sup>. Recently, novel nanoparticles (NPs) are rapidly progressing in both diagnostics and therapeutics fields by proposing merit solutions to many limitations of conventional drugs such as nonspecific targeting and low efficacy<sup>30</sup>. Among all the efficient NPs, most attention has been focused on metal particles with an extensive focus on ZnO QDs and Fe<sub>3</sub>O<sub>4</sub> NPs<sup>31</sup>. The favorable toxicity of zinc NPs for cancer cells and the potent ability of iron NPs to discriminate cancer cells from their normal counterparts encouraged us to bind these NPs to create a multifunctional nanocomposite system capable of killing cancerous cells while inducing minimal cytotoxicity against normal cells<sup>32,33</sup>. Moreover, because of the low solubility of this NP in aqueous media, we used hydroxylated carbon nanotubes (CNT) in the combination of ZnO QD and Fe<sub>3</sub>O<sub>4</sub> in the form of ZnO/CNT@Fe<sub>3</sub>O<sub>4</sub> nanocomposites to increase their water-solubility. The chemical analysis, structure, morphology, and size of ZnO/CNT@Fe<sub>3</sub>O<sub>4</sub> nanocomposite were explored by FTIR, XRD, SEM, and TEM, respectively.

The result of our study demonstrated a significant decrease in viability and metabolic activity of AML derived-KG1 cells after treatment with ZnO/CNT@Fe<sub>3</sub>O<sub>4</sub>. Many studies revealed that the cytotoxicity of these nanomaterials, at least partially, may be induced as a result of reactive oxygen species (ROS) generation, which in turn can promote apoptosis signaling by inducing the expression of multiple pro-apoptotic members of the Bcl2-family of mitochondria-targeting proteins<sup>14,34</sup>. Interestingly, we found that ZnO/CNT@Fe<sub>3</sub>O<sub>4</sub> induces apoptosis in KG1 cells through elevation of the ratio of the pro- to anti-apoptotic genes via alteration of Bax and Bcl-2 expression. Sirelkhatim et al. reported that ZnO NPs could provide signaling that in turn regulates cell cycle progression through induction of G1 or G2/M cell cycle arrest<sup>35</sup>. In agreement, we found that not only ZnO/CNT@Fe<sub>3</sub>O<sub>4</sub> decreased the percentage of cells in the S phase but also blocked the transition of the cells from the G1 phase through increasing the

expression levels of p21 and p27 cyclin-dependent kinase inhibitors. The resulting data also declared that treatment of KG1 cells with ZnO/CNT@Fe<sub>3</sub>O<sub>4</sub> hindered the mRNA expression of the c-Myc proto-oncogene, as the critical regulators of the cell cycle transition from G1 to S phase. In harmony, our recent study on chronic myeloid leukemia K562 cells indicates that the level of c-Myc expression was markedly decreased after treatment with ZnO/CNT@Fe<sub>3</sub>O<sub>4</sub><sup>14</sup>. Moreover, intrigued by the results of a recent study that established the synergistic correlation between ZnO/CNT@Fe<sub>3</sub>O<sub>4</sub> and imatinib on K562 cells<sup>14</sup> (Figure 6). We conducted a synergistic experiment to determine the effects of this nanocomposite on the cytotoxic effects of VCR. Based on the results of combinatorial experiments, ZnO/CNT@Fe<sub>3</sub>O<sub>4</sub> potentiated the cytotoxic effect of VCR against KG1 cells, as the viability and metabolic activity of the cells were lower in combinatorial series than either agent alone. Taken together, the results of the current study shed new light on the promising effects of metal nanoparticles in acute leukemia treatment and re-emphasized the fact that these molecules may have large impacts on cancer treatment strategies, either as a single agent or in combination with chemotherapeutic agents. However, further studies need to be carried out to confirm the safety and usefulness of ZnO/CNT@Fe<sub>3</sub>O<sub>4</sub> in cancer therapeutics.

## ACKNOWLEDGMENTS

The authors would like to express their gratitude to Shahid Beheshti University of Medical Sciences (Tehran, Iran) for supporting this study.

## CONFLICTS OF INTEREST

The authors declare no conflicts of interest.

## REFERENCES

1. Kroschinsky F, Stölzel F, Bonin SV, et al. New drugs, new toxicities: severe side effects of modern targeted and immunotherapy of cancer and their management. *Crit Care*. 2017;21(1):89.
2. Song, X, Peng Y, Wang X, et al. Incidence, survival, and risk factors for adults with acute myeloid leukemia not otherwise specified and acute myeloid leukemia with recurrent genetic abnormalities: analysis of the

- surveillance, epidemiology, and end results (SEER) database, 2001–2013. *Acta Haematol.* 2018;139(2):115-127.
3. Lai C, Doucette K, Norsworthy K. Recent drug approvals for acute myeloid leukemia. *J Hematol Oncol.* 2019;12(1):100.
  4. Medeiros BC, Chan SM, Daver NG, et al. Optimizing survival outcomes with post-remission therapy in acute myeloid leukemia. *Am J Hematol.* 2019;94(7):803-811.
  5. Schirmacher V. From chemotherapy to biological therapy: A review of novel concepts to reduce the side effects of systemic cancer treatment. *Int J Oncol.* 2019;54(2):407-419.
  6. Mi Y, Shao Z, Vang J, et al. Application of nanotechnology to cancer radiotherapy. *Cancer Nanotechnol.* 2016. 7(1):11.
  7. Wang X, Zhang R, Wu C, et al. The application of Fe3O4 nanoparticles in cancer research: a new strategy to inhibit drug resistance. *J Biomed Mater Res A.* 2007;80(4):852-60.
  8. Amreddy N, Babu A, Muralidharan R, et al. Recent advances in nanoparticle-based cancer drug and gene delivery. *Adv Cancer Res.* 2018;137:115-170.
  9. Wang J, Gao S, Wang S, et al. Zinc oxide nanoparticles induce toxicity in CAL 27 oral cancer cell lines by activating PINK1/Parkin-mediated mitophagy. *Int J Nanomedicine.* 2018;13:3441-3450.
  10. Sadri A, Changizi V, Eivazadeh N. Evaluation of glioblastoma (U87) treatment with ZnO nanoparticle and X-ray in spheroid culture model using MTT assay. *Radiat Phys Chem.* 2015. 115: 17-21.
  11. Farasat M, Niazvand F, Khorsandi L. Zinc oxide nanoparticles induce necroptosis and inhibit autophagy in MCF-7 human breast cancer cells. *Biologia.* 2020. 75(1):161-174.
  12. Xie Y, Liu D, Cai C, et al. Size-dependent cytotoxicity of Fe3O4 nanoparticles induced by biphasic regulation of oxidative stress in different human hepatoma cells. *Int J Nanomedicine.* 2016;11:3557-70.
  13. Tanino R, et al. Anticancer Activity of ZnO Nanoparticles against Human Small-Cell Lung Cancer in an Orthotopic Mouse Model. *Mol Cancer Ther.* 2020;19(2):502-512.
  14. Yousefi AM, Safaroghli-Azar A, Fakhroueian Z, et al. ZnO/CNT@ Fe3O4 induces ROS-mediated apoptosis in chronic myeloid leukemia (CML) cells: an emerging prospective for nanoparticles in leukemia treatment. *Artif Cells Nanomed Biotechnol.* 2020;48(1):735-745.
  15. Bashash D, Ghaffari SH, Zaker F, et al. BIBR 1532 increases arsenic trioxide-mediated apoptosis in acute promyelocytic leukemia cells: therapeutic potential for APL. *Anticancer Agents Med Chem.* 2013;13(7):1115-25.
  16. Safaroghli-Azar A, Bashash D, Sadreazami P, et al. PI3K- $\delta$  inhibition using CAL-101 exerts apoptotic effects and increases doxorubicin-induced cell death in pre-B-acute lymphoblastic leukemia cells. *Anticancer Drugs.* 2017. 28(4): 436-445.
  17. Javidparvar A, Ramezanzadeh B, Ghasemi E. Effect of various spinel ferrite nanopigments modified by amino propyl trimethoxy silane on the corrosion inhibition properties of the epoxy nanocomposites. *Corrosion.* 2016. 72(6): 761-774.
  18. Ankamwar B, Thorat A. Rod-shaped magnetite nano/microparticles synthesis at ambient temperature. *Jchem.* 2013.
  19. Zhang Y, Shao L, Liu B, et al. Effect of molecular weight of liquid polysulfide on water and organic solvent resistances of waterborne polyurethane/polysulfide copolymer. *Prog Org Coat.* 2017;112: 75-85.
  20. Jmiai A, El Ebrahimi B, Tara A, et al. Application of Zizyphus Lotuse-pulp of Jujube extract as green and promising corrosion inhibitor for copper in acidic medium. *J Mol Liq.* 2018; 268: 102-113.
  21. Wan S, He F, Wu J, et al. Rapid and highly selective removal of lead from water using graphene oxide-hydrated manganese oxide nanocomposites. *J Hazard Mater.* 2016;314:32-40
  22. Cui M, Ren S, Zhao H, et al. Polydopamine coated graphene oxide for anticorrosive reinforcement of waterborne epoxy coating. *Chem Eng J.* 2018. 335: 255-266.
  23. Li M, Liu Q, Jia Z, et al. *Electrophoretic deposition and electrochemical behavior of novel graphene oxide-hyaluronic acid-hydroxyapatite nanocomposite coatings.* *Appl Surf Sci.* 2013. 284: 804-810.
  24. Javidparvar AA, Naderi R, Ramezanzadeh B, et al. Graphene oxide as a pH-sensitive carrier for targeted delivery of eco-friendly corrosion inhibitors in chloride solution: Experimental and theoretical investigations. *J Ind Eng Chem.* 2019. 72: 96-213.
  25. Sui J, Li J, Li Z, et al. Synthesis and characterization of one-dimensional magnetic photocatalytic CNTs/Fe3O4–ZnO nanohybrids. *Mater Chem Phys.* 2012. 134(1): 229-234.
  26. Olm E, Jönsson-Videsäter K, Ribera-Cortada I, et al. Selenite is a potent cytotoxic agent for human primary AML cells. *Cancer Lett.* 2009; 282(1): 116-123.
  27. Aswathanarayan JB, Vittal RR, Muddegowda U. Anticancer activity of metal nanoparticles and their peptide conjugates against human colon adenorectal carcinoma cells. *Artif Cells Nanomed Biotechnol.* 2018;46(7):1444-1451.
  28. Ostrovsky S, Kazimirsky G, Gedanken A, Brodie C. Selective cytotoxic effect of ZnO nanoparticles on glioma cells. *Nano Research.* 2009;2(11):882-90.

29. Hackl H, Astanina K, Wieser R. Molecular and genetic alterations associated with therapy resistance and relapse of acute myeloid leukemia. *J Hematol Oncol.* 2017;10(1):51.
30. Khandel P, Kumar YR, Kumar SD, et al. Biogenesis of metal nanoparticles and their pharmacological applications: present status and application prospects. *J Nanostructure Chem.* 2018; 8(3): 217-254.
31. Bisht G, Rayamajhi S, Kc B, et al. Synthesis, characterization, and study of in vitro cytotoxicity of ZnO-Fe<sub>3</sub>O<sub>4</sub> magnetic composite nanoparticles in human breast cancer cell line (MDA-MB-231) and mouse fibroblast (NIH 3T3). *Nanoscale Res Lett.* 2016;11(1):537
32. Ostrovsky S, Kazimirsky G, Gedanken A, et al. *Selective cytotoxic effect of ZnO nanoparticles on glioma cells.* *Nano Res.* 2009. 2(11): 882-890.
33. Khan MI, Mohammad A, patil G, et al. Induction of ROS, mitochondrial damage and autophagy in lung epithelial cancer cells by iron oxide nanoparticles. *Biomaterials.* 2012. 33(5): 1477-88.
34. Alarifi S, Ali H, Alkahtani S, et al. *Regulation of apoptosis through bcl-2/bax proteins expression and DNA damage by nano-sized gadolinium oxide.* *Int J Nanomedicine.* 2017;12:4541-4551.
35. Sirelkhatim AH, Mahmoud SH, Seeni A, et al. *Preferential cytotoxicity of ZnO nanoparticle towards cervical cancer cells induced by ROS-mediated apoptosis and cell cycle arrest for cancer therapy.* *J Nanoparticle Res.* 2016. 18(8):219.